International Journal of Research in Medical Sciences
Radder N et al. Int J Res Med Sci. 2025 Oct;13(10):4436-4444
www.msjonline.org
pISSN 2320-6071 | eISSN 2320-6012

DOI: https://dx.doi.org/10.18203/2320-6012.ijrms20252905

Review Article

Meningeal abnormalities: a radiologist's guide to comprehensive imaging and differential diagnosis

Nivedita Radder*, Shrinivas Radder

Department of Radiology, University of Arkansas for Medical Sciences, Little Rock, AR, USA

Received: 16 August 2025
Revised: 02 September 2025
Accepted: 03 September 2025

***Correspondence:**
Dr. Nivedita Radder,
E-mail: nivedita.shirol@gmail.com

ABSTRACT

Meningeal abnormalities encompass a wide spectrum of pathological conditions affecting the protective layers of the central nervous system the dura mater, arachnoid mater, and pia mater. These abnormalities may arise from infectious, neoplastic, inflammatory, traumatic, or post-surgical origins and often present with non-specific clinical symptoms such as headache, seizures, or altered mental status. As such, neuroimaging plays a pivotal role in their evaluation, providing critical information for accurate diagnosis and effective management. This article serves as a comprehensive guide for radiologists, offering a structured approach to the imaging and differential diagnosis of meningeal diseases. It begins with a review of the normal meningeal anatomy, including recent discoveries about the glymphatic system and the fourth meningeal layer, and proceeds to detail the utility of key imaging modalities, particularly magnetic resonance imaging (MRI) and computed tomography (CT), in assessing meningeal pathology. Emphasis is placed on distinguishing between pachymeningeal and leptomeningeal involvement based on enhancement patterns, as well as identifying hallmark imaging signs such as dural thickening, nodular lesions, and enhancement distribution. Common and rare disease entities including meningitis, meningioma, dural metastases, neurosarcoidosis, and carcinomatous meningitis are explored through detailed imaging features and differential considerations. The article also highlights advanced techniques including contrast-enhanced 3D FLAIR, dynamic contrast-enhanced MRI, and emerging applications of artificial intelligence in meningeal evaluation. Through illustrative case examples and a systematic diagnostic framework based on current evidence, this guide aims to enhance radiologists' diagnostic accuracy and clinical confidence, ultimately contributing to more timely and informed management of patients with meningeal abnormalities.

Keywords: Meningeal abnormalities, Meninges, Pachymeninges, Leptomeninges, MRI, CT

INTRODUCTION

The meninges—comprising the dura mater, arachnoid mater, and pia mater—form a critical protective barrier for the central nervous system, serving not only as mechanical shields but also as dynamic interfaces for cerebrospinal fluid (CSF) circulation, immune surveillance, and metabolic homeostasis.[1] Recent advances, including the discovery of a fourth meningeal layer and elucidation of the glymphatic system, have revolutionized our understanding of meningeal pathophysiology.[2] The glymphatic system, consisting of periarterial CSF influx, CSF-interstitial fluid exchange, and perivenous efflux pathways, plays crucial roles in waste clearance and may represent a route for disease propagation.[3]

The spectrum of meningeal pathology encompasses infectious, neoplastic, inflammatory, vascular, and iatrogenic conditions, each manifesting with variable imaging patterns that demand precise radiological interpretation.[4] The fundamental distinction between pachymeningeal (dural) and leptomeningeal (pia-arachnoid) enhancement patterns, while essential for

differential diagnosis, may oversimplify the complex pathophysiological processes involved.[5] Contemporary neuroimaging has evolved significantly beyond conventional sequences, with contrast-enhanced 3D fluid-attenuated inversion recovery (FLAIR) demonstrating superior sensitivity (96% versus 68%) compared to standard T1-weighted imaging for detecting leptomeningeal disease.[6]

Advanced techniques such as dynamic contrast-enhanced magnetic resonance imaging (MRI), susceptibility-weighted imaging (SWI), and PET-MRI fusion have unveiled previously undetectable meningeal abnormalities, offering quantitative biomarkers for disease activity and treatment response.[7] The integration of artificial intelligence and radiogenomics promises to further transform diagnostic accuracy, enabling pattern recognition and molecular phenotype prediction from imaging data alone.[8]

This comprehensive review synthesizes current understanding of meningeal anatomy with practical imaging approaches, critically evaluating traditional enhancement paradigms while integrating recent molecular and genetic insights. We propose a structured framework for navigating the increasingly complex landscape of meningeal disease, emphasizing the importance of clinical correlation and awareness of potential imaging pitfalls in the era of precision medicine.

ANATOMY AND PHYSIOLOGY OF THE MENINGES

The meninges comprise three protective membranes the dura mater, arachnoid mater, and pia mater that surround the brain and spinal cord, serving as structural and physiological barriers for the central nervous system (CNS).[9] Recent discoveries have identified a fourth meningeal layer, termed the subarachnoid lymphatic-like membrane (SLYM), which divides the subarachnoid space into functional compartments and may play crucial roles in immune surveillance (Table 1).[2,10]

The dura mater is the outermost and thickest layer, composed of five distinct layers according to collagen bundle orientation.[11] Within the cranial cavity, it consists of two sublayers: the periosteal layer attached to the skull and the meningeal layer that continues into the spinal canal. The dura creates important folds (falx cerebri, tentorium cerebelli, and diaphragma sellae) that compartmentalize the cranial cavity.[12] Richly innervated by sensory nerves, particularly branches of the trigeminal and vagus nerves, the dura is clinically significant in pain syndromes and is frequently involved in disorders such as subdural hematomas and intracranial hypotension.[13]

The arachnoid mater, a thin avascular membrane, adheres loosely to the dura while creating the subarachnoid space with the underlying pia mater. This space, filled with cerebrospinal fluid and traversed by arachnoid trabeculae and blood vessels, represents a common site for pathological conditions including meningitis and subarachnoid hemorrhage.[14] The recently discovered SLYM layer within this space may regulate CSF flow and immune cell trafficking.[2]

The pia mater, the innermost layer, closely invests the brain and spinal cord, following gyral and sulcal contours. It allows penetration of capillaries and arterioles into the parenchyma through perivascular spaces, which serve as conduits for the glymphatic system.[15] Although nearly invisible on standard imaging, pathological involvement of the pia is crucial in conditions like leptomeningeal carcinomatosis and infectious meningitis.[16]

Functionally, the meninges participate in CSF absorption through arachnoid granulations, act as immunological interfaces via resident macrophages and lymphocytes, and contribute to intracranial pressure regulation.[17] The glymphatic system facilitates waste clearance through convective flow, with impairment linked to neuroinflammation, neurodegeneration, and tumor spread.[3,18] Understanding these anatomical and functional relationships is fundamental for accurate interpretation of meningeal enhancement patterns and selection of optimal imaging protocols.

IMAGING MODALITIES AND TECHNIQUES FOR MENINGEAL ASSESSMENT

Magnetic resonance imaging (MRI) remains the gold standard for evaluating meningeal abnormalities due to its exceptional soft tissue contrast, multiplanar capability, and sensitivity to subtle pathological changes.[19] Post-contrast T1-weighted sequences effectively visualize enhancement patterns, with pachymeningeal enhancement appearing smooth and linear, while leptomeningeal enhancement follows cortical sulci and cisterns.[20]

Contrast-enhanced 3D FLAIR has emerged as a superior technique, with 96% sensitivity for detecting leptomeningeal disease compared to 68% for conventional T1-weighted imaging.[6] The suppression of CSF signal on FLAIR enhances conspicuity of subtle meningeal enhancement, particularly valuable in early meningitis, carcinomatosis, and post-surgical evaluation.[21] Timing of image acquisition is critical, with optimal enhancement typically observed 10-20 minutes after contrast administration.[22]

Computed tomography (CT) serves a vital role in acute neurological emergencies due to rapid acquisition and wide availability. While lacking MRI's soft tissue sensitivity, CT excels at identifying calcifications, acute hemorrhage, and osseous abnormalities.[23] In bacterial meningitis, CT may demonstrate hyperdense exudates in the basal cisterns, while chronic conditions like tuberculous meningitis may show characteristic basal enhancement with calcification.[24]

Table 1: Summary of meningeal layers and their radiologic relevance.

Layer	Location and structure	Key function	Imaging relevance
Dura mater	Outer, thick, fibrous; two layers in the cranium	Mechanical protection; pain-sensitive	Pachymeningeal enhancement; seen in hypotension, metastases
Arachnoid	Middle, thin, avascular; bridges over sulci	Forms subarachnoid space; CSF flow	Leptomeningeal enhancement in meningitis, carcinomatosis
Pia mater	Inner, delicate; follows brain contours	Vascular exchange; CNS interface	Involved in leptomeningeal disease; not seen directly
SLYM	Within subarachnoid space; newly discovered	Immune surveillance; CSF compartmentalization	May influence enhancement patterns; research ongoing

ADVANCED IMAGING TECHNIQUES

Advanced imaging techniques provide additional diagnostic capabilities beyond conventional sequences. Diffusion-weighted imaging (DWI) detects restricted diffusion in purulent exudates with ADC values of 0.3-0.6×10^{-3} mm²/s in bacterial meningitis, markedly restricted diffusion with ADC less than 0.5×10^{-3} mm²/s in empyema, variable restriction based on cellularity in neoplastic infiltration, and restricted diffusion in associated infarcts showing cytotoxic edema.[25] Susceptibility-weighted imaging (SWI) identifies hemorrhage, calcification, and superficial siderosis with high sensitivity.[26] Dynamic contrast-enhanced MRI (DCE-MRI) quantifies blood-brain barrier permeability through pharmacokinetic modeling, with K-trans values correlating with disease activity in inflammatory conditions and extravascular extracellular volume (V_e) increasing in neoplastic infiltration.[27] PET-MRI fusion combines metabolic and anatomical information, particularly valuable in distinguishing active inflammation from fibrosis.[28]

Optimizing protocols requires tailoring sequences to clinical suspicion. A comprehensive meningitis protocol should include pre- and post-contrast T1-weighted, T2-weighted, FLAIR, DWI, and contrast-enhanced 3D FLAIR sequences.[29] For intracranial hypotension, spine imaging with heavily T2-weighted myelography and fat-saturated post-contrast sequences helps identify CSF leaks.[30]

MENINGEAL ENHANCEMENT PATTERNS AND THEIR DIAGNOSTIC IMPLICATIONS

Meningeal enhancement patterns on contrast-enhanced MRI provide crucial diagnostic information for evaluating CNS pathology.[31] These patterns primarily fall into two categories: pachymeningeal and leptomeningeal enhancement (Table 2), though mixed patterns occur in conditions such as neurosarcoidosis and IgG4-related disease.[32]

Pachymeningeal enhancement involves the dura mater and typically presents as smooth, linear, bilateral thickening.[33] In intracranial hypotension, compensatory venous engorgement leads to diffuse smooth enhancement, commonly accompanied by brain sagging (average descent 5.7 mm), subdural effusions (50% of cases), and pituitary enlargement.[34] Dural metastases, frequently from breast (35%), prostate (20%), or lung cancers (18%), manifest as nodular or plaque-like thickening, especially with adjacent bone involvement.[35] Post-surgical enhancement is typically focal, resolving within 6-12 weeks in uncomplicated cases.[36]

Leptomeningeal enhancement affects the pia and arachnoid mater, appearing as thin, curvilinear enhancement following cortical sulci and cisterns.[37] In bacterial meningitis, enhancement is most prominent in the basal cisterns and over convexities, with associated complications including hydrocephalus (30%), infarction (25%), and ventriculitis (15%).[38] Tuberculous meningitis demonstrates characteristic thick, nodular basal enhancement with gelatinous exudates, leading to cranial nerve palsies in 25-50% of cases.[39] Leptomeningeal carcinomatosis presents with diffuse, nodular enhancement in patients with systemic malignancy, with CSF cytology positive in only 50-60% on first examination.[40]

Recent studies utilizing contrast-enhanced 3D FLAIR have identified subtle enhancement patterns previously undetectable on conventional imaging.[41] The "ivy sign" on FLAIR, representing slow flow in leptomeningeal collaterals, helps distinguish moyamoya disease from other causes of leptomeningeal enhancement.[42] Mixed enhancement patterns require careful correlation with clinical findings, CSF analysis, and systemic imaging to establish the diagnosis.[43]

To better illustrate the diagnostic value of these enhancement patterns, Table 3 summarizes key imaging characteristics, enhancement types, and their most common clinical associations.

Differential diagnosis of meningeal abnormalities

The differential diagnosis requires systematic integration of imaging patterns, clinical presentation, CSF findings, and patient demographics.[44] The initial distinction between pachymeningeal and leptomeningeal enhancement significantly narrows diagnostic possibilities.[45]

Table 2: Comparison of pachymeningeal and leptomeningeal enhancement patterns.

Feature	Pachymeningeal enhancement	Leptomeningeal enhancement
Meningeal layers involved	Dura mater only	Arachnoid and pia mater
Appearance on MRI	Smooth, linear, often bilateral	Gyriform, serpentine, follows brain sulci
Typical MRI sequence	Post-contrast T1-weighted	Post-contrast T1-weighted and CE-FLAIR
Common causes	Intracranial hypotension, post-surgery, metastasis	Meningitis, leptomeningeal carcinomatosis, inflammation
Associated findings	Brain sagging, dural thickening	Cortical swelling, CSF abnormalities
Clinical implication	Often benign or secondary	Often urgent and pathological

Table 3: Radiologic features and enhancement patterns in common meningeal diseases.

Condition	Enhancement pattern	MRI features	Common clinical clues
Intracranial hypotension	Pachymeningeal	Smooth dural thickening, brain sagging, venous engorgement	Orthostatic headache, recent lumbar puncture
Post-surgical changes	Pachymeningeal	Focal dural enhancement at surgical site	History of neurosurgery or trauma
Dural metastasis	Pachymeningeal	Nodular dural thickening with bone involvement	Known malignancy, localized neurologic symptoms
Leptomeningeal carcinomatosis	Leptomeningeal	Gyriform/cisternal enhancement, cranial nerve involvement	Systemic cancer, cranial neuropathies
Tuberculous meningitis	Leptomeningeal	Basal cistern enhancement, tuberculomas, infarcts	Immunocompromised state, endemic exposure
Bacterial meningitis	Mixed	Diffuse enhancement with DWI restriction in exudates	Fever, meningismus, elevated CSF WBC
Neurosarcoidosis	Mixed	Nodular basal meningeal enhancement, pituitary involvement	Multisystem disease, elevated ACE, cranial nerve palsy
Fungal meningitis	Leptomeningeal	Gelatinous pseudocysts, nodular enhancement	Immunocompromised, indolent course

Pachymeningeal enhancement differential

Intracranial hypotension (Figure 1) remains the most common cause of diffuse pachymeningeal enhancement, occurring in 4-5 per 100,000 annually.[46] Key imaging features include diffuse smooth dural thickening observed in 100% of cases, brain sagging with tonsillar descent greater than 5 mm in 80% of patients, subdural fluid collections in 50%, venous sinus engorgement in 90%, and pituitary hyperemia in 70% of cases.

Dural metastases present as focal or multifocal nodular enhancement in patients with known malignancy.[47] The most common primary tumors include breast carcinoma accounting for 35% of cases, prostate cancer in 20%, lung cancer in 18%, and hematologic malignancies in 15% of dural metastases. Idiopathic hypertrophic pachymeningitis, though rare (prevalence 0.95 per 100,000), presents with progressive cranial neuropathies and uniform dural thickening showing T2 hypointensity due to fibrosis.[48]

Leptomeningeal enhancement differential

Infectious meningitis represents the most urgent differential consideration.[52] Bacterial meningitis (Figures 2 and 3) presents acutely with prominent basal and convexity enhancement, DWI restriction in purulent exudates, and complications including hydrocephalus in 30% and infarction in 25% of cases.[53] Tuberculous meningitis (Figure 4) demonstrates thick nodular basal enhancement with tuberculomas in 60% of patients, communicating hydrocephalus in 75%, and perforator territory infarcts in 30%.[54] Fungal meningitis shows gelatinous pseudocysts with soap-bubble appearance, particularly in immunocompromised patients, while viral meningitis typically presents with mild enhancement, often normal early imaging, and a self-limiting course.[55,56]

Leptomeningeal carcinomatosis (Figure 5) occurs in 5-10% of patients with systemic malignancy.[57] The most common primary sources are breast cancer in 35% of cases, lung cancer in 25%, melanoma in 20%, and gastrointestinal tumors in 10%.

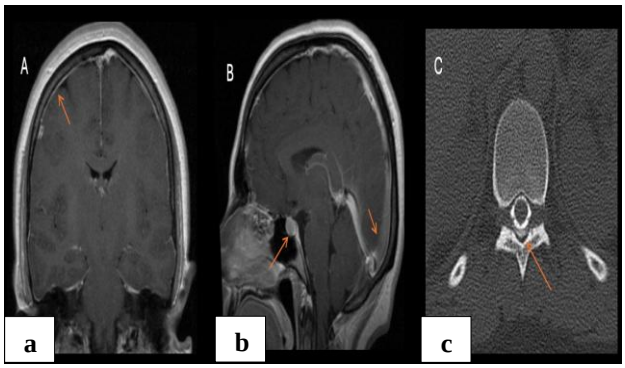

Figure 1: CSF leak-induced intracranial hypotension (a) post-contrast coronal T1 image shows smooth, diffuse pachymeningeal thickening characteristic of low-pressure headache, (b) post-contrast sagittal T1 image demonstrates classic findings of pituitary hyperemia, dilated venous sinuses, and cerebellar tonsillar descent measuring 7 mm, and (c) thoracic CT myelogram reveals posterior epidural contrast accumulation at T8-9 level, indicative of active CSF leak.

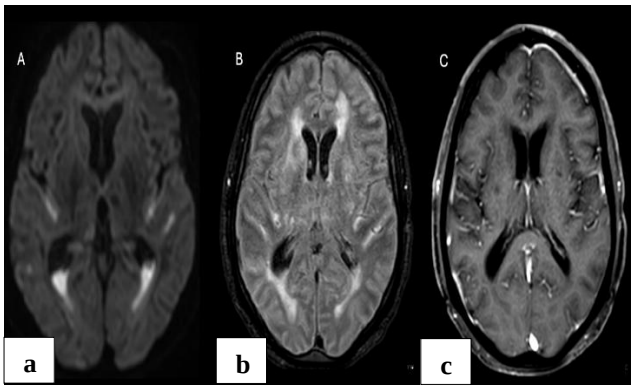

Figure 2: Bacterial meningitis with ventriculitis (a) DWI (b=1000) shows layering, diffusion-restricting debris in bilateral occipital horns (ADC values 0.5×10^{-3} mm^2/s) and Sylvian fissures, (b) FLAIR imaging reveals hyperintense signal in sulcal spaces and ventricular system bilaterally, and (c) T1 post-contrast demonstrates leptomeningeal and ependymal enhancement consistent with meningoventriculitis. CSF analysis showed WBC 2,500/mm^3 with 90% neutrophils.

Neurosarcoidosis

Neurosarcoidosis affects 5-10% of patients with systemic sarcoidosis, presenting with both pachymeningeal and leptomeningeal enhancement (Figure 6).[58] Characteristic features include basilar predominance in 80% of cases, pituitary or hypothalamic involvement in 50%, cranial nerve enhancement in 40%, and associated systemic findings in 90% of patients. Subacute and chronic meningitis may develop, with sarcoidotic leptomeningitis tending to occur around the skull base and potentially extending to the spinal cord meninges. Cranial nerve dysfunction, predominantly peripheral facial palsy, seizures, and communicating hydrocephalus are characteristic of chronic sarcoidosis meningitis. Involvement of other organs occurs frequently, with lungs affected in 90% of systemic sarcoidosis cases, liver in 20-30%, eyes in 10-30%, and lymph nodes in 10-20%, serving as diagnostic indicators.

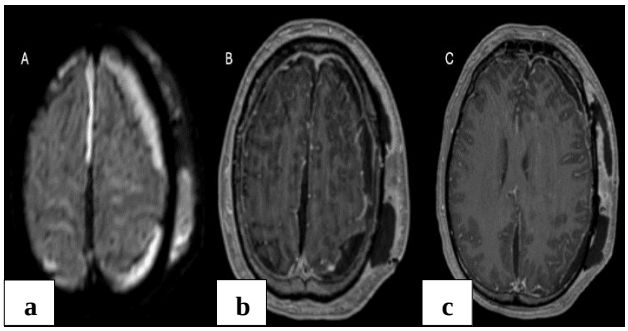

Figure 3: Post-craniotomy meningitis with subdural empyema (a) DWI shows restricted diffusion (ADC 0.4×10^{-3} mm^2/s) in subdural collections along the left hemisphere, right frontal convexity, and interhemispheric fissure, and (b and c) T1 post-contrast sequences reveal peripheral enhancement of subdural collections (empyema), diffuse pachymeningeal and leptomeningeal enhancement (meningitis), and rim-enhancing scalp collection at the operative bed (abscess).

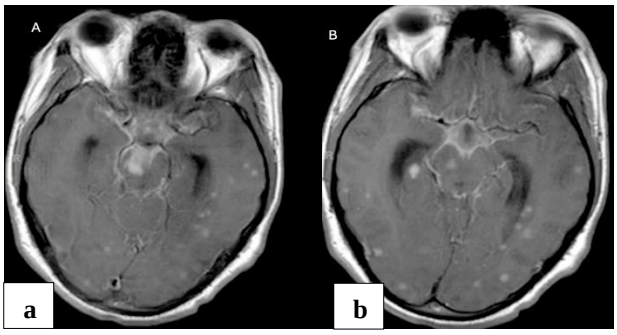

Figure 4: CNS tuberculosis (a and b) axial T1 post-contrast shows basilar meningeal enhancement with multiple enhancing tuberculomas in both hemispheres and midbrain.

Meningiomas

As the most common primary intracranial neoplasm representing 37.6% of primary CNS tumors, meningiomas (Figure 7) present as well-circumscribed, homogeneously enhancing masses.[49] The 2021 WHO classification recognizes 15 subtypes with varying imaging

characteristics.[50] Grade 1 meningiomas, comprising 80% of cases, demonstrate smooth margins with homogeneous enhancement. Grade 2 meningiomas, accounting for 17%, show irregular margins with heterogeneous enhancement, while grade 3 meningiomas, representing 3% of cases, exhibit brain invasion and necrosis. The characteristic "dural tail" sign appears in 72% of cases, while hyperostosis occurs in 20%.[51]

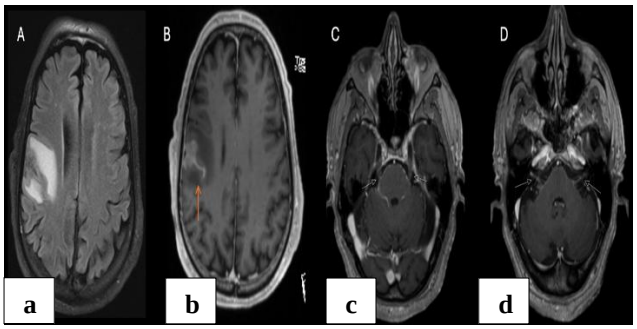

Figure 5: Leptomeningeal carcinomatosis in lung cancer patient (a) FLAIR axial image shows poorly defined hyperintensity in the right posterior frontal lobe, and (b-d) axial T1-weighted post-contrast sequences demonstrate multifocal nodular leptomeningeal enhancement involving the right posterior frontal region and pontine surface. Bilateral enhancement of cranial nerves V, VII, and VIII within the cerebellopontine angle cisterns confirms extensive leptomeningeal metastatic disease.

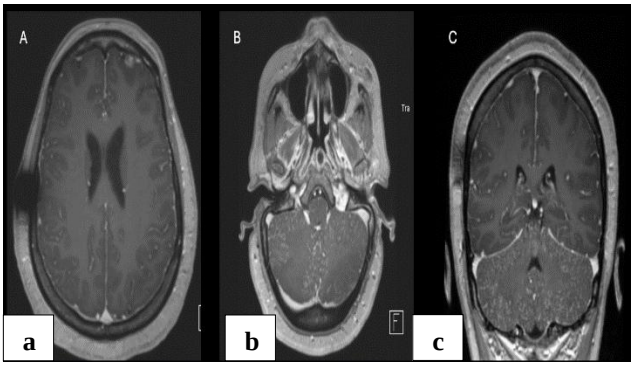

Figure 6: Neurosarcoidosis (a-c) axial and coronal T1 post-contrast imaging shows widespread nodular leptomeningeal thickening with enhancement above and below the tentorium.

ADVANCED IMAGING TECHNIQUES AND FUTURE DIRECTIONS

It is illustrated in Table 4.

Contrast-enhanced 3D FLAIR imaging

Three-dimensional contrast-enhanced FLAIR has revolutionized detection of subtle leptomeningeal pathology.[59] By suppressing CSF signal while preserving contrast enhancement, this technique achieves 96% sensitivity versus 68% for conventional T1-weighted imaging, enables superior detection of early meningitis before clinical symptoms, enhances visualization of leptomeningeal carcinomatosis, and improves evaluation of treatment response.[6] Optimal timing is 10-20 minutes post-contrast, with 1 mm isotropic resolution recommended.[60]

Diffusion-weighted imaging applications

DWI provides critical functional information beyond anatomical detail.[61] In bacterial meningitis, restricted diffusion occurs in purulent exudates with ADC values of $0.3\text{-}0.6\times10^{-3}$ mm²/s. Empyema demonstrates markedly restricted diffusion with ADC values less than 0.5×10^{-3} mm²/s, while neoplastic infiltration shows variable restriction based on cellularity. Associated infarcts display cytotoxic edema with characteristic restricted diffusion patterns. Advanced diffusion techniques including diffusion tensor imaging (DTI) and diffusion kurtosis imaging (DKI) show promise for characterizing microstructural changes.[62]

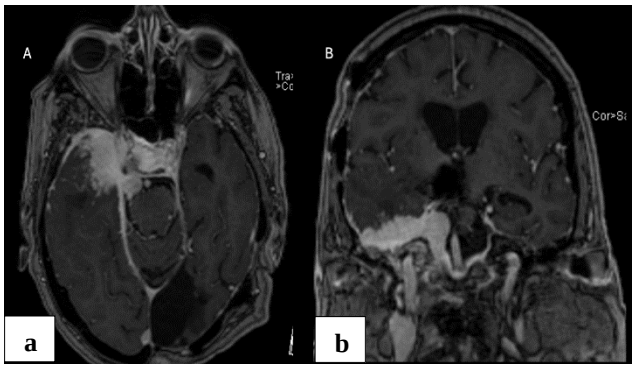

Figure 7: Aggressive meningioma (a and b) post-contrast T1-weighted axial and coronal images reveal a large, homogeneously enhancing, irregularly marginated extra-axial mass at the right central skull base and anterior temporal convexity. The mass demonstrates aggressive features with cavernous sinus invasion and ICA encasement (causing mild narrowing), trans spatial extension through the foramen ovale, and involvement of the sellar, suprasellar, and right prepontine regions. Associated mass effect displaces the right temporal lobe and compresses the right pons.

Dynamic contrast-enhanced MRI

DCE-MRI quantifies blood-brain barrier permeability through pharmacokinetic modeling.[63] K-trans values correlate with disease activity in inflammatory conditions, while extravascular extracellular volume increases in neoplastic infiltration. Permeability maps guide biopsy targeting and serial measurements monitor treatment response, providing valuable quantitative assessment of disease progression and therapeutic efficacy.

PET-MRI fusion imaging

Hybrid PET-MRI combines metabolic and anatomical information.[64] FDG-PET identifies hypermetabolic foci in lymphoma and carcinomatosis, while ^{11}C-methionine PET differentiates tumor from inflammation.[68] Ga-DOTATATE imaging characterizes meningiomas, and amyloid PET tracers detect CAA-related inflammation, offering comprehensive multimodal assessment of meningeal pathology.

Artificial intelligence applications

Machine learning algorithms show promising results.[65] Automated detection achieves 94% accuracy for meningeal enhancement, while pattern classification distinguishes infectious from neoplastic causes. Radiomics extracts quantitative features predicting molecular subtypes, and deep learning algorithms predict treatment response and prognosis, representing the future of personalized meningeal imaging interpretation.

Table 4: Advanced imaging techniques and clinical applications.

Imaging technique	Key application	Diagnostic utility	Limitation
3D contrast-enhanced FLAIR	Early leptomeningeal enhancement	High sensitivity in subarachnoid spaces	Timing dependentand contrast dosage
Diffusion-weighted imaging/ADC mapping	Infection versus tumor differentiation	Quantitative assessment	Motion artifacts
Dynamic contrast-enhanced MRI	BBB permeability quantification	Disease activity monitoring	Complex post-processing required
PET-MRI fusion	Metabolic characterization	Distinguishes active disease	Limited availability and high cost
SWI	Hemorrhage/calcification detection	High sensitivity for blood products	Susceptibility artifacts
AI/Radiomics	Pattern recognition	Automated detection	Requires validation

CONCLUSION

The evaluation of meningeal abnormalities has undergone significant advancements with the evolution of imaging technology and an increased understanding of meningeal pathophysiology. The recent discovery of the SLYM layer and elucidation of the glymphatic system have provided new insights into disease mechanisms and potential therapeutic targets. Contemporary imaging approaches, particularly contrast-enhanced 3D FLAIR and advanced quantitative techniques, enable the detection of previously invisible pathology and provide biomarkers for disease monitoring.

Key principles for optimal meningeal imaging include protocol optimization based on clinical suspicion, recognition of characteristic enhancement patterns, integration of advanced techniques when conventional imaging is equivocal, correlation with clinical findings and CSF analysis, and awareness of potential pitfalls and mimics the integration of artificial intelligence promises to enhance diagnostic accuracy and efficiency further. However, effective diagnosis ultimately requires the synthesis of imaging findings with clinical context by experienced radiologists.

Recommendations

Future directions include the development of molecular imaging probes targeting specific disease mechanisms, the expansion of AI applications for automated detection and characterization, and the integration of imaging biomarkers into clinical trials. The goal remains a timely and accurate diagnosis to enable optimal patient management and improved outcomes. As our understanding of meningeal diseases continues to expand, imaging will play an increasingly central role not only in diagnosis but also in guiding precision therapy and monitoring treatment response.

Funding: No funding sources
Conflict of interest: None declared
Ethical approval: Not required

REFERENCES

1. Kurokawa R, Kurokawa M, Isshiki S, Harada T, Nakaya M, Baba A, et al. Dural and Leptomeningeal Diseases: Anatomy, Causes, and Neuroimaging Findings. RadioGraphics. 2023;43(9):e230039.
2. Møllgård K, Beinlich FRM, Kusk P, Miyakoshi LM, Delle C, Plá V, et al. A mesothelium divides the subarachnoid space into functional compartments. Science. 2023;379(6627):84-8.
3. Kamagata K, Andica C, Takabayashi K, Saito Y, Taoka T, Nozaki H, et al. Association of MRI indices of glymphatic system with amyloid deposition and cognition in mild cognitive impairment and Alzheimer disease. Neurology. 2022;99(24):e2648-60.
4. Smirniotopoulos JG, Murphy FM, Rushing EJ, Rees JH, Schroeder JW. Patterns of contrast enhancement in the brain and meninges. RadioGraphics. 2007;27(2):525-51.
5. Singh SK, Leeds NE, Ginsberg LE. MR imaging of leptomeningeal metastases: comparison of three

sequences. AJNR Am J Neuroradiol. 2002;23(5):817-21.
6. McKinney AM, Palmer CA, Short J, Lucato LT, Truwit CL. Detection of leptomeningeal disease using contrast-enhanced 3D FLAIR MR imaging. AJNR Am J Neuroradiol. 2007;28(4):691-9.
7. Tofts PS, Brix G, Buckley DL, Evelhoch JL, Henderson E, Knopp MV, et al. Estimating kinetic parameters from dynamic contrast-enhanced T1-weighted MRI of a diffusable tracer: standardized quantities and symbols. J Magn Reson Imaging. 1999;10(3):223-32.
8. Yamada I, Baradaran H, Gupta A. Artificial intelligence in brain tumor imaging: applications and challenges. Neuroradiology. 2021;63(10):1501-14.
9. Weller RO. Microscopic morphology and histology of the human meninges. Morphologie. 2005;89(284):22-34.
10. Mastorakos P, McGavern D. The anatomy and immunology of vasculature in the central nervous system. Sci Immunol. 2019;4(37):eaav0492.
11. Sakka L, Coll G, Chazal J. Anatomy and physiology of cerebrospinal fluid. Eur Ann Otorhinolaryngol Head Neck Dis. 2011;128(6):309-16.
12. Netter FH. Atlas of Human Anatomy. 7th edition. Philadelphia: Elsevier. 2018.
13. Gray H, Standring S. Gray's Anatomy: The Anatomical Basis of Clinical Practice. 42nd edition. Philadelphia: Elsevier. 2020.
14. Mortazavi MM, Quadri SA, Khan MA, Gustin A, Suriya SS, Hassanzadeh T, et al. Subarachnoid trabeculae: A comprehensive review. World Neurosurg. 2018;111:279-90.
15. Iliff JJ, Wang M, Liao Y, Plogg BA, Peng W, Gundersen GA, et al. A paravascular pathway facilitates CSF flow through the brain parenchyma. Sci Transl Med. 2012;4(147):147ra111.
16. Duvernoy HM. The Human Brain: Surface, Three-Dimensional Sectional Anatomy with MRI, and Blood Supply. 2nd edition. Vienna: Springer-Verlag. 1999.
17. Johanson CE, Duncan JA 3rd, Klinge PM, Brinker T, Stopa EG, Silverberg GD. Multiplicity of cerebrospinal fluid functions. Cerebrospinal Fluid Res. 2008;5:10.
18. Rasmussen MK, Mestre H, Nedergaard M. The glymphatic pathway in neurological disorders. Lancet Neurol. 2018;17(11):1016-24.
19. Atlas SW. Magnetic Resonance Imaging of the Brain and Spine. 5th ed. Philadelphia: Lippincott Williams & Wilkins. 2016.
20. Provenzale JM, Mukundan S, Dewhirst M. The role of blood-brain barrier permeability in brain tumor imaging. AJR Am J Roentgenol. 2005;185(3):763-7.
21. Hakyemez B, Yildirim N, Erdogan C, Kocaeli H, Korfali E, Bekar A. Evaluation of different types of meningeal enhancement on post-contrast FLAIR images. Eur J Radiol. 2006;60(3):450-5.
22. Mathews VP, Caldemeyer KS, Lowe MJ, Greenspan SL, Weber DM, Ulmer JL. Brain: gadolinium-enhanced fast fluid-attenuated inversion-recovery MR imaging. Radiology. 1999;211(1):257-63.
23. Toh CH, Wei KC, Ng SH, Wan YL, Lin CP, Castillo M. Differentiation of brain abscesses from necrotic glioblastomas and cystic metastatic brain tumors with diffusion tensor imaging. AJNR Am J Neuroradiol. 2011;32(9):1646-51.
24. Jinkins JR, Gupta R, Chang KH, Rodriguez-Carbajal J. MR imaging of central nervous system tuberculosis. Radiol Clin North Am. 1995;33(4):771-86.
25. Schaefer PW, Grant PE, Gonzalez RG. Diffusion-weighted MR imaging of the brain. Radiology. 2000;217(2):331-45.
26. Haacke EM, Xu Y, Cheng YC, Reichenbach JR. Susceptibility weighted imaging (SWI). Magn Reson Med. 2004;52(3):612-8.
27. O'Connor JP, Jackson A, Parker GJ, Jayson GC. DCE-MRI biomarkers in the clinical evaluation of antiangiogenic and vascular disrupting agents. Br J Cancer. 2007;96(2):189-95.
28. Chen W, Silverman DH. Advances in evaluation of primary brain tumors. Semin Nucl Med. 2008;38(4):240-50.
29. Rossi A, Severino M. Pediatric meningeal disorders: what the neuroradiologist needs to know. Neuroimaging Clin N Am. 2015;25(1):1-24.
30. Schievink WI. Spontaneous spinal cerebrospinal fluid leaks and intracranial hypotension. JAMA. 2006;295(19):2286-96.
31. Meltzer CC, Fukui MB, Kanal E, Smirniotopoulos JG. MR imaging of the meninges. Part I: Normal anatomic features and nonneoplastic disease. Radiology. 1996;201(2):297-308.
32. Stern BJ, Royal W 3rd, Gelfand JM, Clifford DB, Tavee J, Pawate S, et al. Definition and consensus diagnostic criteria for neurosarcoidosis. JAMA Neurol. 2018;75(12):1546-53.
33. Mokri B. The Monro-Kellie hypothesis: applications in CSF volume depletion. Neurology. 2001;56(12):1746-8.
34. Mokri B. Spontaneous cerebrospinal fluid leaks: from intracranial hypotension to cerebrospinal fluid hypovolemia. Mayo Clin Proc. 1999;74(11):1113-23.
35. Gavrilovic IT, Posner JB. Brain metastases: epidemiology and pathophysiology. J Neurooncol. 2005;75(1):5-14.
36. Macdonald DR, Cascino TL, Schold SC Jr, Cairncross JG. Response criteria for phase II studies of supratentorial malignant glioma. J Clin Oncol. 1990;8(7):1277-80.
37. Glass JP, Melamed M, Chernik NL, Posner JB. Malignant cells in cerebrospinal fluid: the meaning of positive CSF cytology. Neurology. 1979;29(10):1369-75.
38. van de Beek D, Cabellos C, Dzupova O, Esposito S, Klein M, Kloek AT, et al. ESCMID guideline: diagnosis and treatment of acute bacterial meningitis. Clin Microbiol Infect. 2016;22(Suppl 3):S37-62.

39. Thwaites GE, van Toorn R, Schoeman J. Tuberculous meningitis: more questions, still too few answers. Lancet Neurol. 2013;12(10):999-1010.
40. Le Rhun E, Weller M, Brandsma D, Van den Bent M, de Azambuja E, Henriksson R, et al. EANO-ESMO Clinical Practice Guidelines for diagnosis, treatment and follow-up of patients with leptomeningeal metastasis from solid tumours. Ann Oncol. 2017;28(suppl_4):84-99.
41. Singh SK, Agris JM, Leeds NE, Ginsberg LE. Intracranial leptomeningeal metastases: comparison of depiction at FLAIR and contrast-enhanced MR imaging. Radiology. 2000;217(1):50-3.
42. Mori N, Mugikura S, Higano S, Kaneta T, Takahashi S, Takahashi K, et al. The leptomeningeal "ivy sign" on fluid-attenuated inversion recovery MR imaging in Moyamoya disease. AJNR Am J Neuroradiol. 2009;30(5):930-5.
43. Taillibert S, Chamberlain MC. Leptomeningeal metastasis. Handb Clin Neurol. 2018;149:169-204.
44. Castillo M, Mukherji SK. Imaging of the pediatric head, neck, and spine. Philadelphia: Lippincott-Raven. 1996.
45. Whiteman M, Bhattacharya JJ. Imaging of meningitis and ventriculitis. Clin Radiol. 2005;60(10):1105-15.
46. Schievink WI. Spontaneous intracranial hypotension. N Engl J Med. 2021;385(23):2173-8.
47. Nayak L, Abrey LE, Iwamoto FM. Intracranial dural metastases. Cancer. 2009;115(9):1947-53.
48. Kupersmith MJ, Martin V, Heller G, Shah A, Mitnick HJ. Idiopathic hypertrophic pachymeningitis. Neurology. 2004;62(5):686-94.
49. Wiemels J, Wrensch M, Claus EB. Epidemiology and etiology of meningioma. J Neurooncol. 2010;99(3):307-14.
50. Louis DN, Perry A, Wesseling P, Brat DJ, Cree IA, Figarella-Branger D, et al. The 2021 WHO Classification of Tumors of the Central Nervous System: a summary. Neuro Oncol. 2021;23(8):1231-51.
51. Goldbrunner R, Minniti G, Preusser M, Jenkinson MD, Sallabanda K, Houdart E, et al. EANO guidelines for the diagnosis and treatment of meningiomas. Lancet Oncol. 2016;17(9):e383-91.
52. Roos KL, van de Beek D. Bacterial meningitis. Handb Clin Neurol. 2010;96:51-63.
53. Mook-Kanamori BB, Geldhoff M, van der Poll T, van de Beek D. Pathogenesis and pathophysiology of pneumococcal meningitis. Clin Microbiol Rev. 2011;24(3):557-91.
54. Sanei Taheri M, Karimi MA, Haghighatkhah H, Pourghorban R, Samadian M, Delavar Kasmaei H. Central nervous system tuberculosis: an imaging-focused review. Radiol Res Pract. 2015;2015:202806.
55. Perfect JR, Dismukes WE, Dromer F, Goldman DL, Graybill JR, Hamill RJ, et al. Clinical practice guidelines for the management of cryptococcal disease. Clin Infect Dis. 2010;50(3):291-322.
56. Wright WF, Pinto CN, Palisoc K, Baghli S. Viral (aseptic) meningitis: a review. J Neurol Sci. 2019;398:176-83.
57. Batool A, Kasi A. Leptomeningeal Carcinomatosis. In: StatPearls. Treasure Island (FL): StatPearls Publishing. 2023.
58. Bradshaw MJ, Pawate S, Koth LL, Cho TA, Gelfand JM. Neurosarcoidosis: pathophysiology, diagnosis, and treatment. Neurol Neuroimmunol Neuroinflamm. 2021;8(6):e1084.
59. Fukuoka H, Hirai T, Okuda T, Shigematsu Y, Sasao A, Kimura E, et al. Comparison of the added value of contrast-enhanced 3D fluid-attenuated inversion recovery and magnetization-prepared rapid acquisition of gradient echo sequences in relation to conventional postcontrast T1-weighted images for the evaluation of leptomeningeal diseases at 3T. AJNR Am J Neuroradiol. 2010;31(5):868-73.
60. Zivadinov R, Ramasamy DP, Vaneckova M, Gandhi S, Chandra A, Hagemeier J, et al. Leptomeningeal contrast enhancement is associated with disability progression and grey matter atrophy in multiple sclerosis. Neurol Neuroimmunol Neuroinflamm. 2017;4(6):e398.
61. Teksam M, Casey SO, Michel E, Zabramski J, Yaksel D. Diffusion-weighted MR imaging in acute bacterial meningitis. Neuroradiology. 2004;46(6):435-40.
62. Jensen JH, Helpern JA. MRI quantification of non-Gaussian water diffusion by kurtosis analysis. NMR Biomed. 2010;23(7):698-710.
63. Covarrubias DJ, Luetmer PH, Campeau NG. Posterior reversible encephalopathy syndrome: prognostic utility of quantitative diffusion-weighted MR images. AJNR Am J Neuroradiol. 2002;23(6):1038-48.
64. Fitsiori A, Fornecker LM, Simon L, Karentzos A, Garibotto V, Omoumi P, et al. Imaging spectrum of Bing-Neel syndrome. Eur Radiol. 2019;29(1):102-14.
65. Lambin P, Rios-Velazquez E, Leijenaar R, Carvalho S, van Stiphout RG, Granton P, et al. Radiomics: extracting more information from medical images using advanced feature analysis. Eur J Cancer. 2012;48(4):441-6.

Cite this article as: Radder N, Radder S. Meningeal abnormalities: a radiologist's guide to comprehensive imaging and differential diagnosis. Int J Res Med Sci 2025;13:4436-44.